Hydrolytic Degradation Behavior of Poly(butylene succinate)s with Different Crystalline Morphologies

KILWON CHO, JAEYOUNG LEE, KWANWOOK KWON

Department of Chemical Engineering and Environmental Engineering, Polymer Research Institute, Division of Electrical and Computer Engineering, Pohang University of Science and Technology, Pohang 790-784, Korea

Received 14 September 1999; accepted 28 December 1999

ABSTRACT: The effect of crystalline morphology on the hydrolytic degradation behavior of poly(butylene succinate) (PBS) in an alkaline solution was investigated by using scanning electron microscopy, gel permeation chromatography, and weight loss measurement. Morphological changes were induced on PBS samples by different thermal treatments (i.e., melt quenching or isothermal crystallization) at a constant overall degree of crystallinity. It was found that even with a similar degree of crystallinity, the hydrolytic degradation rate of an isothermally crystallized sample at 60°C was higher than that of a melt-quenched sample. This was due to the difference in the internal morphology of the spherulites: the internal structure of spherulite in an isothermally crystallized sample consists of coarse and loosely packed fibrils whereas a melt-quenched sample contains finer and tightly packed fibrils. This result suggested that the internal structure of the spherulite of PBS samples plays an important role in the hydrolytic degradation for this experimental condition. © 2000 John Wiley & Sons, Inc. J Appl Polym Sci 79: 1025–1033, 2001

Key words: hydrolytic degradation; biodegradation; poly(butylene succinate); crystalline morphology

INTRODUCTION

There is growing interest in developing biodegradable polymers for at least two reasons: one is the serious environmental problem of plastic wastes; the other is the effective medical application of biodegradable polymers. Biodegradable polymers are degraded to low molecular weight compounds because of water or the action of the enzymes excreted by microorganisms. Aliphatic polyesters, such as poly(butylene succinate) (PBS), poly(ϵ-caprolactone) (PCL), poly(β-hydroxybutyrate) (PHB), and poly(lactic acid), are known to be biodegradable polymers that can be easily decomposed by the cleavage of ester bond linkage in an acidic or basic condition.[1,2]

It is known that factors affecting biodegradation behavior are polymer structures such as stereochemistry, hydrophilicity, flexibility of chains, and polymer morphology such as the crystallinity, size, form, and number of crystallites.[3–8] Selective chemical degradation of semicrystalline polymers shows certain characteristic changes. During degradation, the crystallinity of the samples increases rapidly at first, then levels off to a much slower rate.[9] This is attributed to the eventual disappearance of the amorphous portions of the samples. Actually, the effect of the crystallinity and morphology of PCL on the enzymatic degradation of its films was studied by several research groups.[10–12] They showed that the degradation first takes place at the amorphous regions prior to the degradation of the crystalline regions. Also,

Correspondence to: K. Cho (kwcho@postech.ac.kr).

Contract grant sponsor: Ministry of Education Research Funds for BK21.

Journal of Applied Polymer Science, Vol. 79, 1025–1033 (2001)

the size, shape, and number of the crystallites have a pronounced effect on the chain mobility of the amorphous regions and thus the rate of the degradation. This was demonstrated by studying the effects of changing the orientation (via stretching) on the degradation. Mochizuki et al.[13] reported the effects of the draw ratio on enzymatic degradation of PCL fibers by *Rhizopus arrhizus* lipase. Their results showed that the enzyme preferentially attacked amorphous or less ordered regions, which permits easier access for the enzyme to the polymer chain, rather than crystalline or more ordered regions of the PCL fiber.

Hydrolytic degradation of polymers is also affected by the polymer morphology that controls the diffusion of water into the polymer matrix: water penetrates at a higher rate in the amorphous region than in the crystalline region, which results in a higher hydrolysis rate in the amorphous region. However, the study of the influence of crystalline morphology on hydrolytic degradation was limited to several specific polymers.[14–16] Moreover, the effect of the microstructure of crystalline morphology, such as the size, form, and internal structure of crystallites, on hydrolytic degradation is not precisely understood so far.

PBS is used for biodegradable polymers because of its hydrolytic degradation behavior in acidic or basic conditions. Also, PBS has a high crystallization rate, so the crystalline microstructure can be easily controlled by changing the crystallization conditions and subsequent thermal treatment, which maintains similar crystallinity. Therefore, in order to study the effect of the microstructure of crystalline morphology on hydrolytic degradation, we chose PBS and prepared the PBS samples with different thermal histories. This study analyzed the crystalline microstructure of PBS in accordance with its thermal history, and its relation with hydrolytic degradation behavior was investigated.

EXPERIMENTAL

Materials and Sample Preparation

The PBS was received from SK Chemicals Inc. (number-average molecular weight = 45,000). PBS granules were thoroughly dried under a vacuum at 50°C for 3 days. The granules of PBS were melted in the mold at 150°C for 5 min, and then the molten polymer films were quenched in ice water or quickly transferred onto a hot stage set at specific temperatures (25 or 60°C); then they crystallized for 72 h. The melt-quenched sample was also annealed at 75°C for 5 days. The thickness of the sample was about 1 mm.

Hydrolytic Degradation

The hydrolytic degradation of the PBS samples was carried out in a 1*N* NaOH solution at 25°C. The dimension of the samples was $1 \times 5 \times 40$ mm. The samples and solution were incubated in a beaker and put in a water bath with gentle shaking. After a fixed period of time the samples were picked out and washed with distilled water and dried to a constant weight in a vacuum oven at 30°C for weighing.

Measurements

The thermal properties of the PBS samples were determined by a differential scanning calorimetry (DSC) instrument (Perkin–Elmer DSC 7) at a scanning rate of 10°C/min. The internal morphology of the spherulite was observed by using a polarized optical microscope (Zeiss Axioplan Microscope). For that purpose, a piece of the sample was embedded using an epoxy resin on a clean glass slide and then polished to a thin, light transparent film. The size and lamellar ordering of the spherulite was obtained by using light scattering apparatus. An He-Ne laser of 632.8-nm wavelength was applied vertically to the film specimen. An H_v geometry was employed in which the optical axis of the analyzer was set perpendicular to that of the polarizer. The angular distribution of the light scattering intensity was detected by a highly sensitive CCD camera and photomultiplier tube. Wide angle X-ray scattering (WAXS) analysis of samples was carried out using a MAC Sciences HF-MX18F X-ray diffractometer in the 2θ range of 10–50° at a scan rate of 4°/min. Small angle X-ray scattering (SAXS) analysis of samples was also carried out using a Philips PW1700 X-ray diffractometer in the 2θ range of 0.1–3.0° at a scan rate of 0.05°/min. The wavelength of the X-ray beam was 0.154 nm (Cu Kα).

After hydrolytic degradation, the surface of the samples was examined with a scanning electron microscope (Hitachi S-4200). The samples were coated with a thin layer of gold and platinum. The change in the molecular weight of the samples before and after hydrolytic degradation was detected by a gel permeation chromatography (GPC) instrument (Waters 600E) calibrated using standard polystyrene at room temperature. Chlo-

Table I Thermal Properties and Solid Structure of PBS with Different Thermal Histories

Sample	Crystal. Temp. (°C)	T_m (°C)	ΔH_m (J/g)	Crystal.[a] (%)	LP[b] (nm)	LT[c] (nm)	R_{H_v} (μm)	P_r[d]
Que[e]	Ice quenched	113.9	63.4	56.1	8.10	5.11	21.5	3.25
Iso-25	25	113.9	63.7	56.4	9.25	5.92	26.2	1.53
Iso-60	60	113.9	68.3	60.4	9.35	5.95	23.6	1.47
Que-Ann[f]	Annealed	113.7	78.4	69.4	9.40	6.00		

[a] The bulk crystallinity was calculated from the DSC.
[b] The long period was estimated from the Lorentz-corrected SAXS intensities as a function of the scattering vector.
[c] The lamellar thickness was estimated from the 1-dimensional correlation function according to the pseudo-two-phase model.
[d] The ordering parameter was calculated by using eq. (2).
[e] The sample was first quenched in ice water after melting, then stored for 2 weeks at room temperature.
[f] The ice-quenched sample was annealed in a vacuum oven at 75°C for 3 days.

roform was used as an eluent at a flow rate of 0.8 mL/min.

RESULTS AND DISCUSSION

Crystalline Structure

It is well known that semicrystalline polymers often show different crystalline structures after different thermal histories.[17–19] In this study, four different PBS samples with different thermal histories were prepared: crystallized isothermally at different temperatures (25 and 60°C) after melting (melt quenched), subsequently annealed at 25°C for 2 weeks, and melt quenched and annealed at 75°C for 5 days.

The morphology and thermal properties of the PBS samples were determined by a polarized optical microscope, DSC, light scattering, WAXS, and SAXS. The crystallinity of the annealed samples was 69%, which was higher than those of melt-quenched or isothermally crystallized samples (56–60%), as expected. However, the difference of crystallinity between melt-quenched and isothermally crystallized samples (25 or 60°C) was not so large, which might be attributed to the high crystallization rate of PBS. The thermal properties and other solid structures of PBS samples with different thermal histories are summarized in Table I.

Figure 1 shows DSC thermograms of the PBS samples prepared by different thermal treatments. The thermograms show typical double melting behavior. Multiple melting behavior is well known in the melting of some semicrystalline polymers such as polypropylene and aliphatic polyesters, which might be attributed to the difference in crystal size, discrete bunching of crystallites of varying degrees of perfection, or melting and recrystallization of some microcrystals.[20–22] In Figure 1 the position of the higher melting peak dose not change for all samples. However, the peak position and the shape of the lower melting peak is different: for isothermally crystallized samples the shape of the lower melting peak is clear whereas for melt-quenched samples the lower peak is smaller and vague. This result indicates that the microcrystalline structure is different for the samples prepared by different thermal histories. The crystalline structure of the PBS samples was further characterized by X-ray scattering experiments, light scattering, and polarized optical microscopy.

Figure 2 shows typical WAXS profiles of PBS with various thermal histories. The positions of the maximum peaks do not change and the shapes of the peaks are very similar. This result

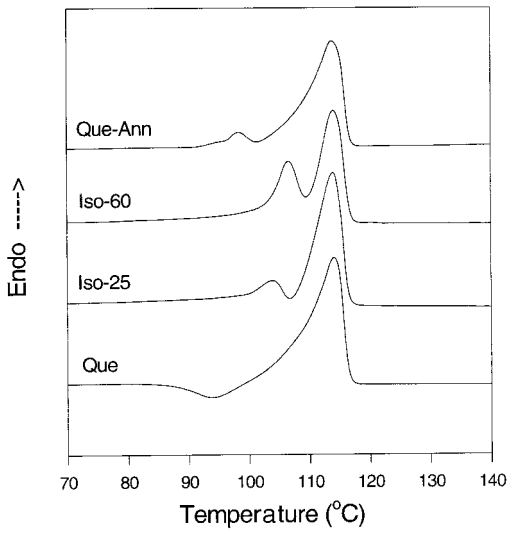

Figure 1 DSC thermograms of PBS crystallized at different temperatures.

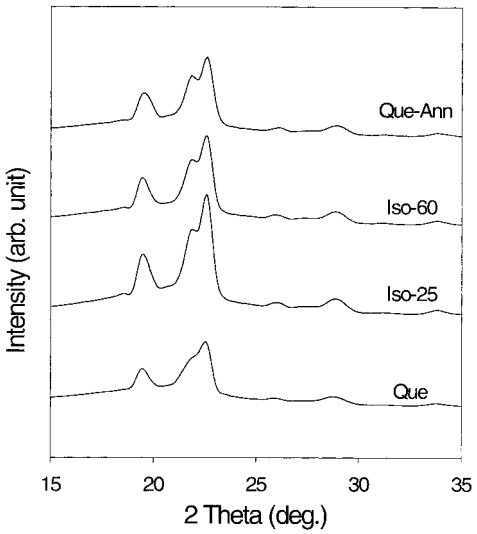

Figure 2 WAXS intensity profiles as a function of 2θ for PBS crystallized at different temperatures.

indicates that the crystal form of PBS (i.e., monoclinic[23]) was not changed by the thermal treatments used in this experiment. Also, the microstructure of the crystals such as the lamellar thickness and the long period was further characterized by using a SAXS technique. The lamellar thickness of the samples was determined from the scattering data according to the pseudo-two-phase model using a 1-dimensional (1-D) correlation function.[24] The lamellar thickness for the melt-quenched sample was 5.1 nm, and the isothermally crystallized and annealed samples showed a slightly higher value of 6.0 nm. The lamellar thickness was not changed much by changing the crystallization condition and thermal history.

The spherulitic nature of PBS samples crystallized at different temperatures is revealed by the H_v light scattering patterns shown in Figure 3. The four-leaf clover pattern in the H_v mode is characteristic of the spherulite, and this pattern is ascribed to the ordering of the optical axis in both the tangential and radial directions within the spherulite.[25] In the melt-quenched sample a clear four-leaf clover pattern appears whereas isothermally crystallized samples do not show this clear pattern. This change of pattern indicates that the optical axis orientation of isothermally crystallized samples is more disordered within the spherulite than that of the melt-quenched sample. Also, based upon 1-D H_v scattering profiles at an azimuthal angle of 45° in the scattering patterns (Fig. 4), one can analyze the details of the spherulite morphology in the following manner. The average radius of the spherulite (R_{H_v}) can be estimated by using the following equation[26,27]:

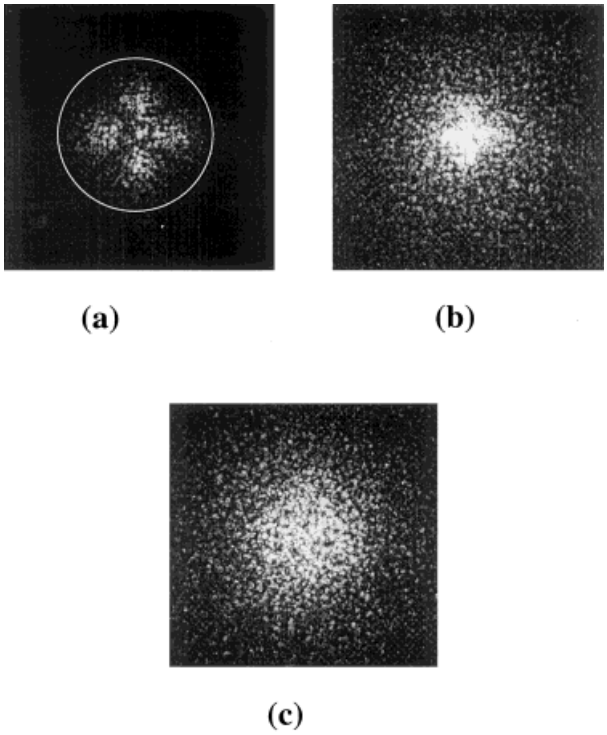

Figure 3 The H_v light scattering patterns of PBS samples crystallized at different temperatures. The circle indicates a scattering angle of 3.6°: (a) melt quenched, (b) isothermally crystallized at 25°C, and (c) isothermally crystallized at 60°C.

$$4.1 = 4\pi(R_{H_v}/\lambda)\sin(\theta_m/2) \quad (1)$$

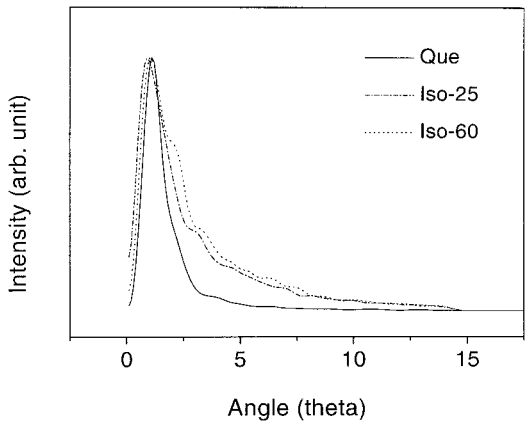

Figure 4 The H_v light scattering profiles normalized by the maximum intensity at an azimuthal angle μ = 45°.

where λ is the wavelength of the light in the medium and θ_m is the peak angle at the maximum intensity. The estimated radii of the PBS spherulites with thermal histories are shown in Table I. The radius of the spherulite is about 20–30 μm and the difference in the radius of the spherulite with thermal histories is not so large. This may be attributed to the high crystallization rate of PBS.

By a 1-D H_v scattering profile, one can also obtain information on the ordering in the spherulite. To discuss the degree of ordering within the spherulite, it is convenient to employ an ordering parameter P_r. According to Yoon and Stein,[25] the relative intensity of scattered light at a small angle ($\theta < \theta_m$) is enhanced by the angular disorder of the optic axis orientation but at a wide angle ($\theta > \theta_m$) it is enhanced by the radial disorder. The P_r is given by using the following equation:

$$P_r = I_{H_v}(\omega = 4)/I_{H_v} \quad (\omega = 8) \tag{2}$$

$$\omega = (2\pi/\lambda)R_{H_v}\sin\theta \tag{3}$$

where ω is the reduced scattering angle. The calculated results of the P_r for PBS samples are also summarized in Table I. Compared with the melt-quenched sample, the isothermally crystallized samples have a lower ordering like that observed by a 2-D scattering pattern. This means that isothermally crystallized samples have a higher random orientation of the lamellar crystals within the spherulite. At present, it is not clear why the lamellae crystallized at a higher temperature have more random orientation. But, this phenomenon leads us to assume that when the lamellae within the spherulite are crystallized at a high temperature, their growth would have a much greater probability of taking a randomness of orientation compared to low temperature crystallization. This speculation is consistent with the observed morphology of the spherulite in a polarized optical micrograph as shown in Figure 5.

The polarized optical microscopic observation on the morphology of spherulites is shown in Figure 5. The diameter of the spherulites is about 40–50 μm, irrespective of the thermal histories, which is in good agreement with the light scattering data (Table I). However, in the photographic pattern of spherulites there is a clear difference between isothermally crystallized samples and the melt-quenched one (Fig. 5). In the melt-quenched sample, a clear Maltese cross pattern

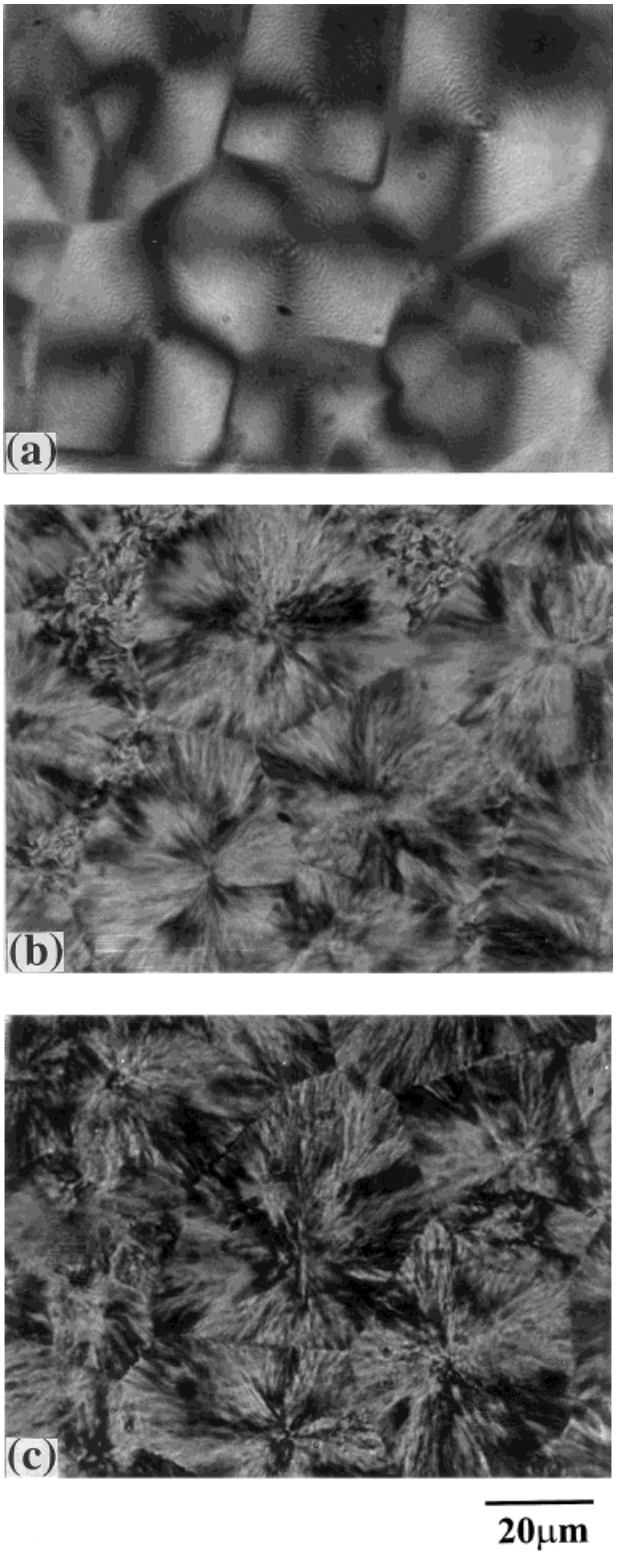

Figure 5 Polarized optical micrographs of PBS samples crystallized at different temperatures: (a) melt quenched, (b) isothermally crystallized at 25°C, and (c) isothermally crystallized at 60°C.

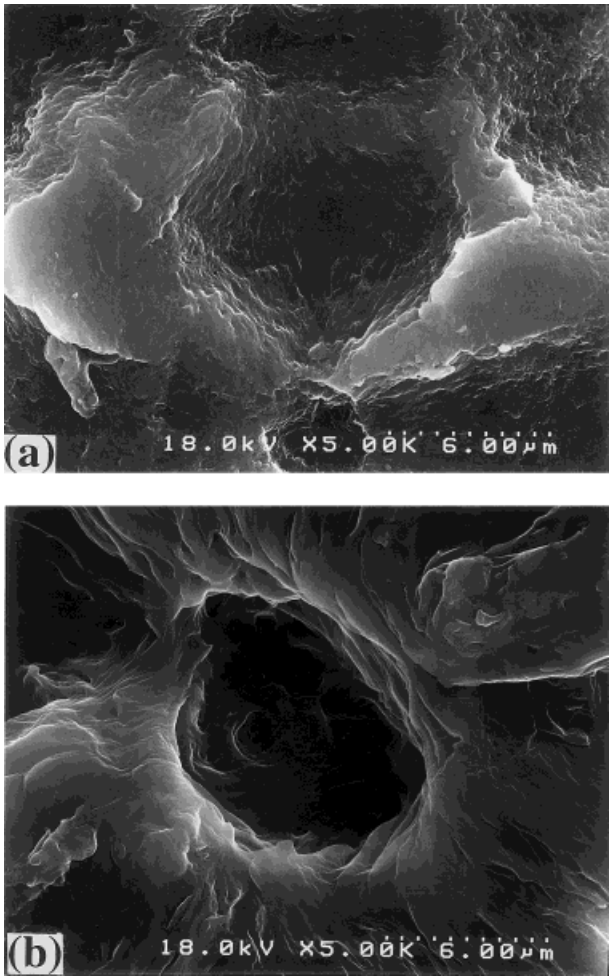

Figure 6 Scanning electron microscopy photographs showing the degradation pattern for the center portion of the spherulite after hydrolysis for 9 days: (a) melt quenched and (b) isothermally crystallized at 25°C.

appears [Fig. 5(a)] whereas isothermally crystallized samples do not show this clear pattern. This particular pattern of the spherulite in the optical microscopic observation is closely related to the internal morphology of the spherulite, such as its lateral size, packing density, and branching of fibrils (bundles of lamellae).

Keith and Padden reported that the internal morphology of a spherulite is determined by the magnitude of the parameter $\sigma = D/G$, where D is the diffusion coefficient for noncrystallizable impurities in the melt and G is the radial growth rate of the spherulite.[28–30] According to their theory, it would be expected that as σ decreases, the texture of the spherulite would become finer, be more densely packed, and have branched fibrils; conversely, as σ increases the texture of the spherulite would become thicker, be less densely packed, and have no branched fibrils. In our experiment the σ value of the melt-quenched sample, which has a high growth rate and a low diffusion coefficient, is considerably lower compared to that of isothermally crystallized samples. Therefore, it can be assumed that internal fibrils of the spherulite for the melt-quenched sample are finer and the spherulites are more densely packed than isothermally crystallized samples. This speculation is verified indirectly by making a comparison of the hydrolytic degradation pattern for each sample (Fig. 6).

Degraded surfaces show quite a different surface morphology after hydrolysis. Fine fibrils were observed on the degraded surface for the melt-quenched sample, [Fig. 6(a)], whereas only thick fibrils were observed in the isothermally crystallized sample [Fig. 6(b)]. The pattern of erosion observed during hydrolysis could reflect the size and shape of fibrils composed of spherulites. Therefore, the internal structure of the spherulite for different thermal histories could be inferred from the degraded morphology (i.e., the melt-quenched spherulite contains finer and more densely packed fibrils). Also, our experimental observations on spherulitic morphology were in good agreement with the extensive series of experimental observations by Keith and Padden.[28–30]

Hydrolytic Degradation

The effects of crystallinity and morphology on polymer hydrolysis were studied for a de-

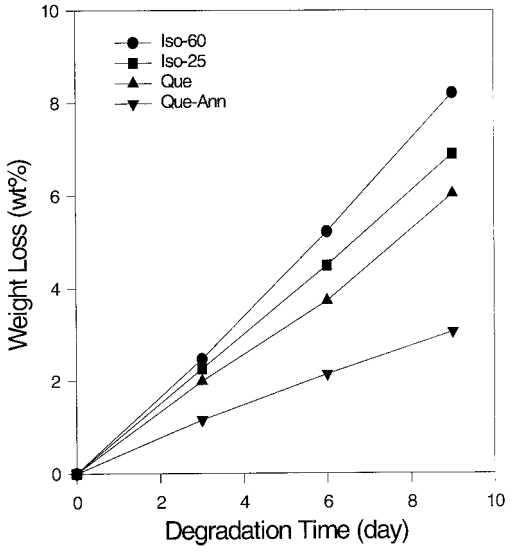

Figure 7 The weight loss of PBS samples crystallized at different temperatures as a function of hydrolysis time in the 1*N* NaOH solution.

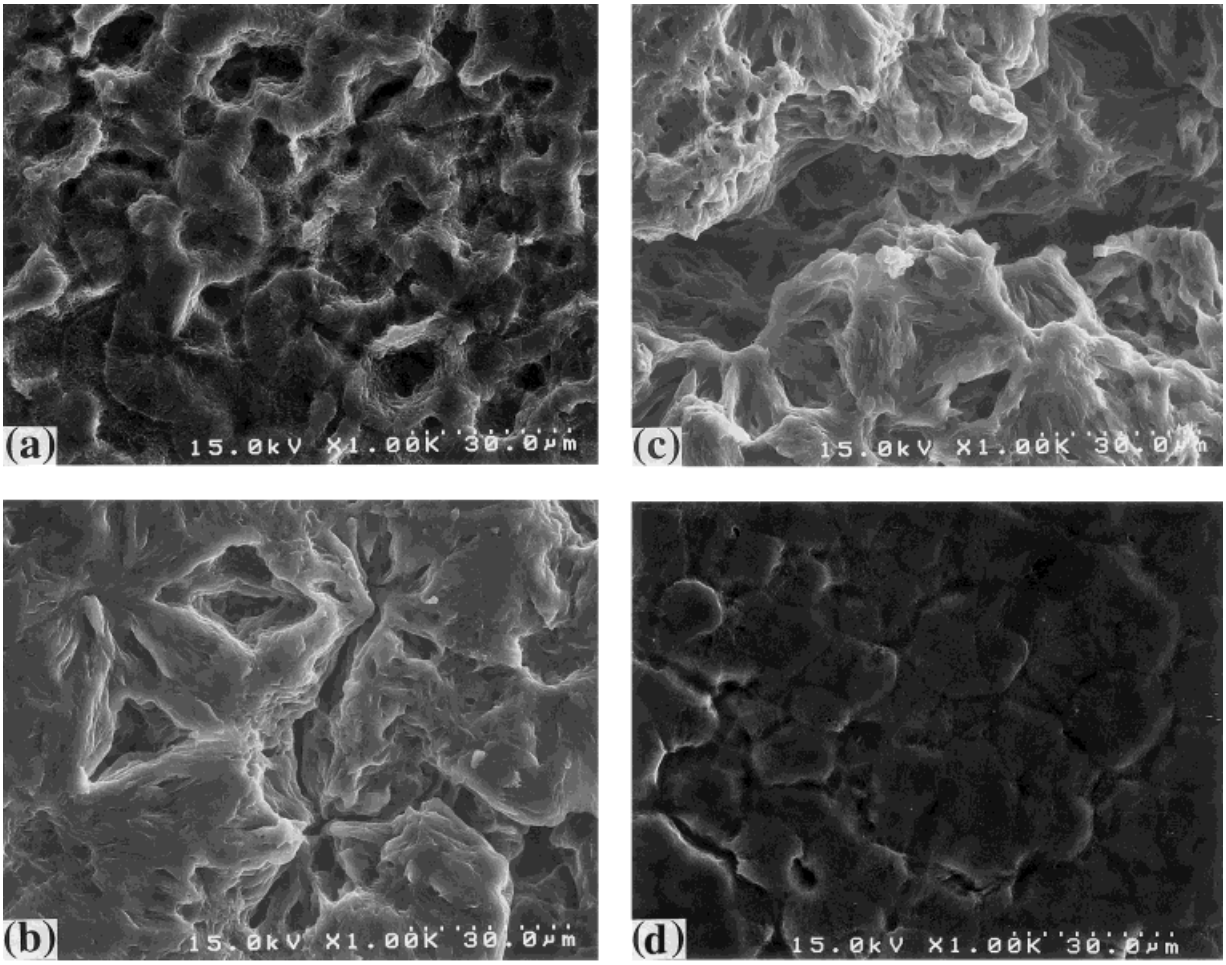

Figure 8 Scanning electron microscopy photographs of the degraded surface of PBS samples crystallized at different temperatures after hydrolysis for 9 days: (a) melt quenched, (b) isothermally crystallized at 25°C, (c) isothermally crystallized at 60°C, and (d) melt quenched and annealed at 75°C.

cade.[14–16] It is known that hydrolytic degradation proceeds at a higher rate in the amorphous region than in the crystalline region. The higher degradation rate in the amorphous region is attributed to the easy diffusion of water molecules into the interior of polymers. Figure 7 shows the weight loss of PBS samples with various thermal histories during hydrolytic degradation. The degradation rate of annealed samples (Que-Ann, crystallinity 69%) was slower than those of nonannealed samples (Que, Iso-25, and Iso-60, crystallinity 56–60%). This result indicates that the crystallinty of a PBS sample plays an important role in determining the hydrolysis rate. This result further supports the conclusion that the hydrolytic degradation takes place preferentially in the amorphous region rather than in the crystalline region. In the case of similar crystallinity (56–60%), the degradation rate of a melt-quenched sample was lower than that of an isothermally crystallized sample at 60°C. The difference in the degradation rate for these samples was considerably large, in spite of similar crystallinity. This result may be related to the structure of crystalline morphology.

Figure 8 shows the scanning electron micrographs of specimen surfaces after hydrolysis for 9 days. The surface of the degraded samples has lost smoothness. As a consequence of hydrolysis, a spherulitic texture is clearly observed. Most of the degraded surfaces are covered with spherulites. These micrographs reveal that the central part of the spherulites and spherulitic impinging lines are degraded first, followed by the other parts of the spherulites. Thus, holes and deeply eroded cracks are observed at both the central part and circumferencial part of the spherulites. This may be explained as being due to the fact that water

molecules penetrate more easily in the center and circumference of the spherulites, which have less ordered chain conformation than in any other part. As a result, preferential hydrolytic degradation took place in these regions. Similar experimental results were reported in the enzymatic biodegradation of PHB by PHB depolymerase.[31] It is interesting that the pattern of hydrolytic degradation for the PBS spherulites was really similar to that of the enzymatic degradation of the PHB spherulites. This result might be attributable to the preferential degradation of the disordered region by water or enzymes.

Careful observation of the degraded surfaces of the specimens with different thermal histories showed that the degradation pattern of the surface for the melt-quenched sample [Fig. 8(a)] was different from those for isothermally crystallized samples [Fig. 8(b,c)]: in the melt-quenched sample, the degraded surface had fine bundles of lamellae and the depth of degradation from the surface was not so deep. However, for isothermally crystallized samples, fine bundles of lamellae in and around the spherulite were not observed on the surface and the depth of erosion was very deep. The explanation may be that the pattern of surface degradation for the PBS was affected by the degree of fibrillar packing in the spherulite. According to the SAXS and optical microscopy results, the spherulite of the melt-quenched sample was composed of densely packed fine fibrils [Fig. 5(a)], so water molecules did not penetrate deeply into the interior of the bulk from the surface in the NaOH solution. Thus, the hydrolysis and erosion for the melt-quenched sample may have occurred step by step from the surface [Fig. 8(a)]. On the other hand, isocrystallized samples had loosely packed thick fibrils, and water molecules penetrated into the samples more deeply compared with the melt-quenched one, so that the surface of the spherulite was dug out more deeply and roughly. Especially in the case of the isocrystallized sample at 60°C, the erosion of the surface was so extensive that the form of the spherulite almost disappeared [Fig. 8(c)].

Figure 9 is a schematic diagram showing water penetration from the surface of the sample and the resulting degradation pattern for the melt-quenched and isothermally crystallized samples, respectively. Ultimately, this change of degradation pattern that arose from the degree of fibrillar packing was closely related to the difference in the hydrolysis rate for PBS samples with different thermal histories as shown in Figure 7.

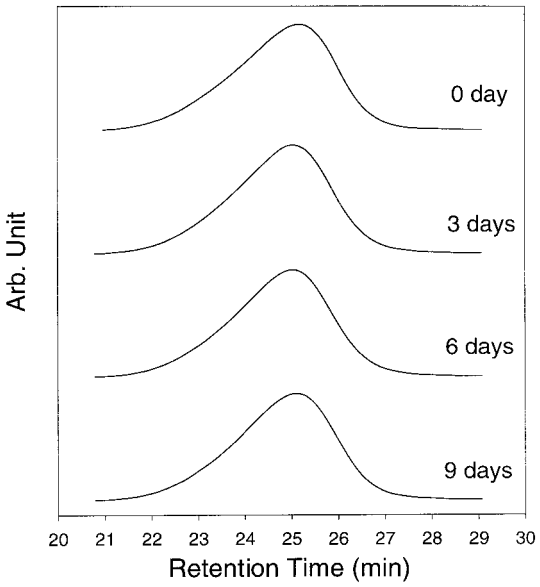

Figure 10 GPC diagrams of the interior of the degraded samples as a function of the hydrolysis time. The sample is melt-quenched PBS.

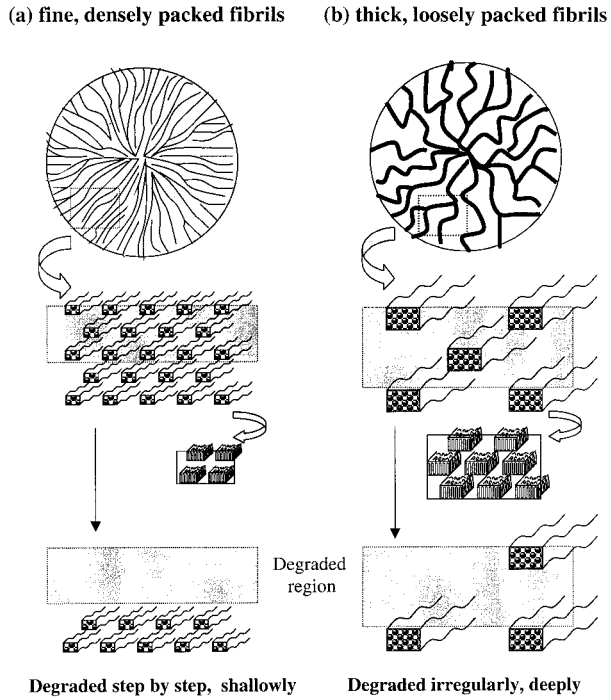

Figure 9 Schematic diagrams showing the course of hydrolysis for PBS samples crystallized at different temperatures for the same amount of time. The shadow portion indicates the domain for water penetration from the surface: (a) melt-quenched sample (fine, densely packed fibrils) and (b) isothermally crystallized sample at 60°C (thick, loosely packed fibrils).

Figure 10 is the GPC diagram obtained by using samples taken from the interior of the degraded specimen. The samples for this GPC experiment were taken from the bulk of the degraded specimens and did not contain the degraded surface. The GPC diagrams showed that the molecular weight distribution of the PBS sample was not changed with degradation time. This result directly showed that the hydrolytic degradation of PBS progressed because of the surface reaction at this experimental condition. We assumed that water diffusion into the bulk of the specimen was restricted by the high crystallinity of PBS.

CONCLUSIONS

A solid structure analysis and hydrolytic degradation of melt-crystallized PBS were conducted. The internal structure of the PBS spherulite was successfully controlled by applying different thermal histories without appreciably altering the overall degree of crystallinity. The annealed sample having higher cyrstallinity showed a lower degradation rate. This result implied that hydrolytic degradation took place preferentially in the amorphous part of the PBS sample and supported the conclusion that the crystallinity of a sample plays a major role in hydrolytic degradation. It was also found that an isothermally crystallized sample at 60°C, which had a spherulite composed of less densely packed fibrils, showed a higher degradation rate compared to a melt-quenched sample, in spite of similar crystallinity. This result indicated that the internal structure of the spherulite also played an important role in hydrolytic degradation. We also found that the hydrolysis of PBS progressed because of a surface reaction in this experimental condition.

REFERENCES

1. Chandra, R.; Rvstgi, R. Prog Polym Sci 1998, 23, 273.
2. Hocking, P. J. J Mol Sci Rev Macromol Chem Phys 1992, C32, 35.
3. Abe, H.; Matsubara, I.; Doi, Y. Macromolecules 1995, 28, 844.
4. Reeve, M. S.; McCarthy, S. P.; Downey, M. J.; Gross, R. A. Macromolecules 1994, 27, 825.
5. Mochizuki, M.; Mukai, K.; Yamada, K.; Ichise, N.; Murase, S.; Iwaya, Y. Macromolecules 1997, 30, 7403.
6. Pitt, C. G.; Gu, Z. W.; Ingram, P.; Hendren, R. W.; J Polym Sci Part A Polym Chem 1987, 25, 955.
7. Abe, H.; Doi, Y.; Aoki, H.; Akehata, T. Macromolecules 1998, 31, 1791.
8. Koyama, N.; Doi, Y. Macromolecules 1997, 30, 826.
9. Spyros, A.; Kimmich, R.; Briese, B. H.; Jendrossek, D. Macromolecules 1997, 30, 8218.
10. Cook, W. J.; Cameron, J. A.; Bell, J. P.; Huang, S. J. J Polym Sci Polym Lett Ed 1981, 19, 159.
11. Jar, P.; Huang, S. J.; Bell, J. P.; Cameron, J. A.; Benedict, C.V. Org Coat Appl Polym Sci Proc 1982, 47, 45.
12. Benedict, C. V.; Cook, V. J.; Jarrett, P.; Cameron, J. A.; Huang, S. J.; Bell, J. P. J Appl Polym Sci 1983, 28, 327.
13. Mochizuki, M.; Hirano, M.; Kanmuri, Y.; Kudo, K.; Tokiwa, Y. J Appl Polym Sci 1995, 55, 289.
14. Tsuji, H.; Ikada, Y. J Appl Polym Sci 1997, 63, 855.
15. Vert, M.; Li, S. M.; Garreau, H. J Controlled Release 1991, 6, 15.
16. Gam, D.; Hyan, S. M.; Ikada, Y. Biomaterials 1995, 16, 833.
17. Bell, J. P.; Dumbleton, J. H. J Polym Sci Part A-2 1969, 7, 1033.
18. Sweet, G. E.; Bell, J. P. J Polym Sci Part A-2 1972, 10, 1273.
19. Bell, J. P.; Slade, P. E.; Dumbleton, J. H. J Polym Sci Part A-2 1968, 6, 1773.
20. Samuels, R. J. J Polym Sci Polym Phys 1975, 13, 1417.
21. Pae, K. D. J Polym Sci A-2 1968, 6, 657.
22. Guerra, G.; Petraccone, V.; Corradini, P.; De-Rosa, C.; Napolitano, R.; Pirozzi, B.; Giunchi, G. J Polym Sci Polym Phys 1984, 22, 1029.
23. Tadokoro, H. Molecular Structure and Properties; Butterworths: London, 1972; p 42.
24. Vonk, C. G. J Appl Cryst 1973, 8, 8122.
25. Yoon, D.; Stein, R. J Polym Sci 1974, 12, 763.
26. Stein, R.; Rhodes, M. J Appl Phys 1960, 31, 1873.
27. Charoensirisomboon, P.; Saito, H.; Inoue, T.; Weber, M.; Koch, E. Macromolecules 1998, 31, 4963.
28. Keith, H. D.; Padden, F. J., Jr. J Appl Phys 1963, 34, 2409.
29. Keith, H. D.; Padden, F. J., Jr. J Appl Phys 1964, 35, 1270.
30. Keith, H. D.; Padden, F. J., Jr. J Appl Phys 1964, 35, 1286.
31. Tomasi, G.; Scandola, M.; Briese, B, H.; Jendrossek, D. Macromolecules 1996, 29, 507.